ACS Sustainable Chemistry & Engineering

pubs.acs.org/journal/ascecg

Research Article

Sustainable, Efficient, and Scalable Preparation of Pure and Performing Spiro-OMeTAD for Perovskite Solar Cells

Sara Mattiello, Giulia Lucarelli, Adiel Calascibetta, Lorenzo Polastri, Erika Ghiglietti, Suresh Kumar Podapangi, Thomas M. Brown, Mauro Sassi, and Luca Beverina*

Cite This: *ACS Sustainable Chem. Eng.* 2022, 10, 4750−4757

Read Online

ACCESS | Metrics & More | Article Recommendations | Supporting Information

ABSTRACT: The technology of organometal halide perovskites is on the verge of the lab to fab transition due to particularly high efficiencies and low cost of the raw materials employed in the active later. The hole transport layer is a key enabling component of such solar cells and at the same time the one requiring more significant synthetic efforts. Alternative materials with improved sustainability are under constant development, yet 2,2′,7,7′-tetrakis(N,N-di(4-methoxyphenyl)amino)-9,9′-spirobifluorene (Spiro-OMeTAD) still represents the standard in the field. We show that the combination of solventless approaches, chemistry on water, and micellar catalysis gives access to such critical material in a fully sustainable, scalable, and efficient way. Performances are validated in devices delivering results equal to those with standard commercial Spiro-OMeTAD but greatly reducing the overall E-factor—a green chemistry metric measuring the waste/purified product ratio of a synthesis, from 5299 to 555, as well as eliminating chlorinated solvents and hazardous chemicals.

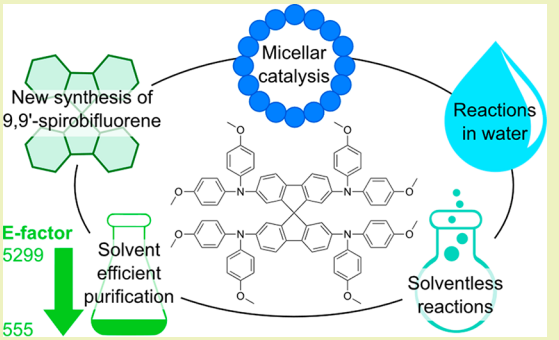

KEYWORDS: *Micellar catalysis, Reactions in water, E-Factor, Hole transporting material, Perovskite solar cells*

INTRODUCTION

Solar cells based on organometal halide perovskites have been very important for third generation photovoltaics.[1] They combine solution-processing fabrication techniques with power conversion efficiencies that almost reach those of silicon.[2] Such remarkable performances are the result of the careful optimization of all the components of the multistacked ensemble constituting the final device. Literature reports show a wide variety of assembly techniques and device architectures,[3] yet the presence of an efficient hole transport layer (HTL) is a frequent feature. In the vast majority of the cases, the material of choice is the well-established Spiro-OMeTAD. Originally proposed as an HTL to be applied in organic monolayer-modified TiO_2 heterojunctions,[4] the popularity of such a 9,9′-spirobifluorene derivative has grown enormously, first as solid state HTL for dye-sensitized solar cells[5−7] and more recently since the introduction of perovskite solar cells.[8] Figure 1 shows the rapid increase in the number of papers citing the use of Spiro-OMeTAD as an HTL which have been published over the past decade. Despite its wide applicability and commercial availability, there is very active research in finding more sustainable and cheaper alternatives.[6,7,9,10]

The literature access to Spiro-OMeTAD is problematic on several respects. As is shown in Scheme 1, the first hurdle is the synthesis of 9,9′-spirobifluorene, requiring the use of hazardous Grignard or organolithium reagents over either 2-bromo[11] or 2-iodo biphenyl (Suppporting Information, Section 2).[12,13]

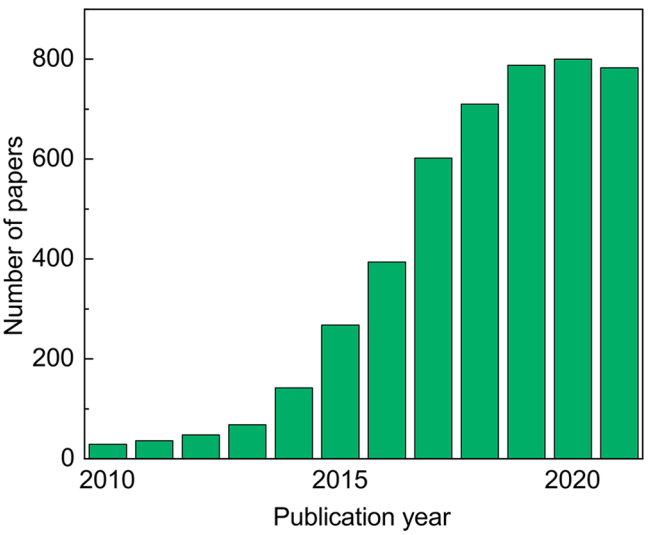

Figure 1. Publications per year in the 2010−2021 period involving the use of Spiro-OMeTAD as the HTL layer. Source SciFinder (as of December 2021).

Received: January 24, 2022
Revised: March 17, 2022
Published: March 31, 2022

Scheme 1. Example of Established Literature Accesses to Spiro-OMeTAD (Top, Black) and Green Chemistry Compliant Route Described in This Paper (Bottom, Green)

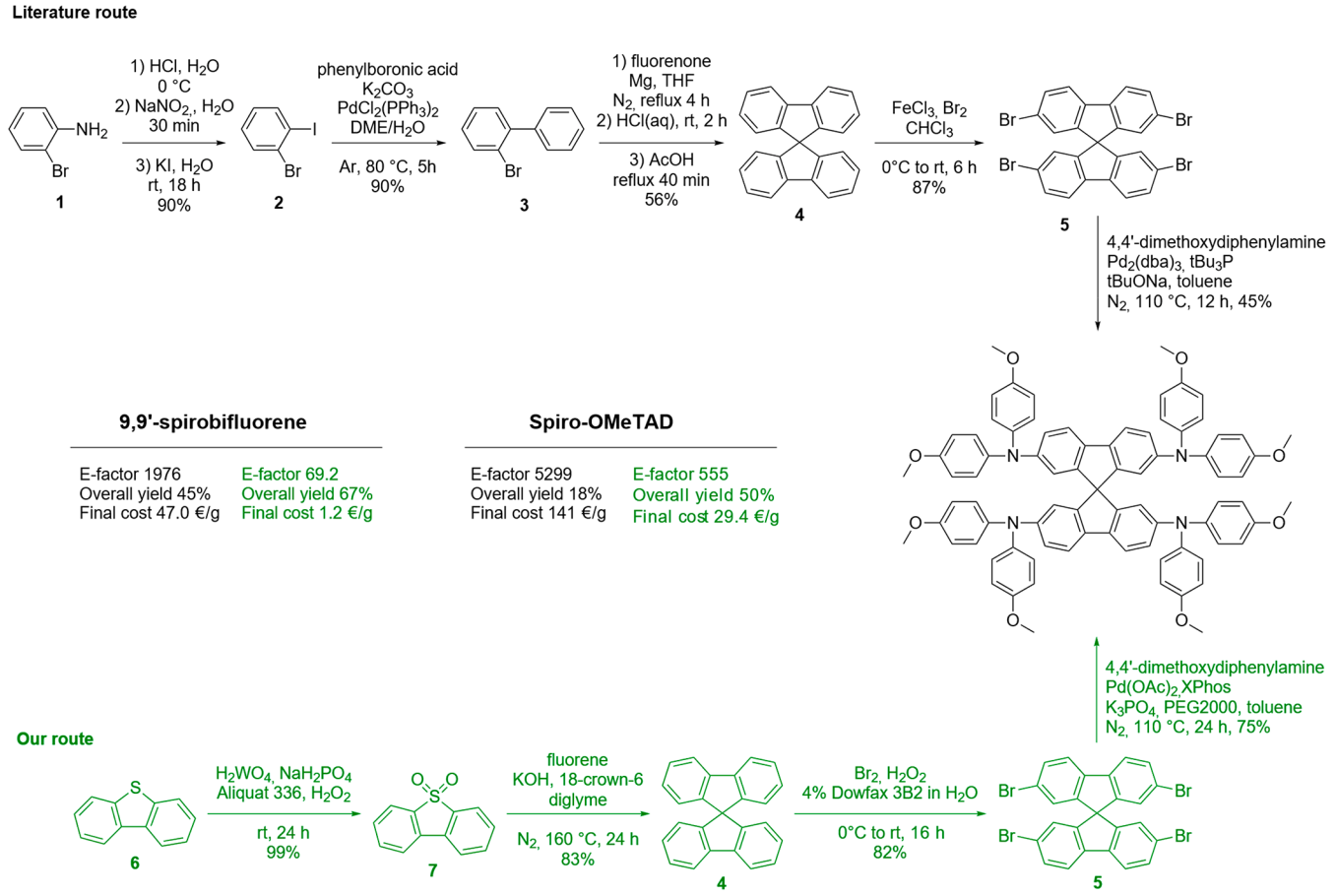

2-Halogenobiphenyl derivatives are themselves poor intermediates requiring a multistep synthesis characterized by poor atom economy. The subsequent bromination is efficient but requires the use of a particularly obnoxious chlorinated solvent.[12] Lastly, 2,2′,7,7′-tetrabromo-9,9′-spirobifluorene is converted in the final product via palladium-catalyzed Buchwald−Hartwig amination with excess 4,4′-dimethoxydiphenylamine. The reaction has only a moderate yield (45%) and requires the use of toluene as the solvent, and the achievement of a suitable purity for applications in devices requires a laborious chromatographic purification impacting in the overall organic solvent's consumption.[14]

The literature suggests several different metrics to quantitatively evaluate the overall impact of a synthetic protocol, including the popular but somewhat limited atom economy.[15] The E-factor, a parameter corresponding to the weight ratio between the waste produced and the purified product, offers additional crucial information.[16] The most relevant quantity included in the E-factor but not in the atom economy is the amount of solvent employed. In the pharmaceutical industry, where synthetic complexity is highest, accepted E-factor values for scaled processes are in the order of a few hundreds.[17] As is detailed in Section 1 of the Supporting Information, the E-factor for the established synthesis of Spiro-OMeTAD is over 5000, a particularly disappointing value.[9] Moreover, the protocol requires toxic solvents and hazardous, pyrophoric materials.

By far the best way to dramatically reduce the E-factor is the removal of organic solvents, frequently accounting for over 90% of the total waste. Water would be the ideal substitute, if not for the hydrophobicity of most organic species. Yet, the last 20 years witnessed a dramatic increase in the number of processes based on water as the solvent, regardless of the water solubility of reagents and products.[18−21] Solventless reactions are also becoming increasingly relevant.[22]

In this paper, we show that it is possible to dramatically reduce both the cost and the environmental impact of the Spiro-OMeTAD synthesis, by drastically reducing organic solvents needed for both synthesis and purification. To these aims, we fully exploit the whole toolbox of green chemistry by developing solventless, micellar, and plain water processes. Our results show that the new synthetic route enables an order of magnitude reduction in cost and E-Factor (from 5299 to 555), and it is scalable and does not compromise the performances.

We tested the materials prepared according to the new route in the preparation of thin film hybrid perovskite solar cells with results in line with those that can be obtained with reference, commercially available samples. Remarkably, we devise an original purification procedure providing Spiro-OMeTAD batches free from organic contaminants (as assessed by NMR and elemental analysis) and featuring a particularly small residual concentration of metal catalysts. The presence of metal impurities is a known factor influencing performances of organic semiconductors in both photovoltaic and field effect transistor devices.[23] In our cases, purification rather than

https://doi.org/10.1021/acssuschemeng.2c00493
ACS Sustainable Chem. Eng. 2022, 10, 4750−4757

directly enhancing performances sizably improved durability with respect to the control sample prepared with commercial HTL.

EXPERIMENTAL SECTION

Materials and Methods. Reagents and solvents were bought from Fisher Scientific, Fluorochem, or Sigma-Aldrich. Filtration on Celite was performed using Celite 353. Filtration on carbon was performed using DARCO activated charcoal (moisture content < 12%, 100 mesh particle size). Compositions of solvent mixtures used as eluents are indicated as volume/volume ratios. NMR spectra were collected on a Bruker NMR Avance 400 NEO. Melting points were determined using a Buchi M-560 apparatus.

Dibenzothiophene-S,S-dioxide (7). Dibenzothiophene (10.00 g, 54.27 mmol), H_2WO_4 (0.135 g, 0.543 mmol), NaH_2PO_4 (65.1 mg, 0.543 mmol), and Aliquat 336 (0.235 g, 0.543 mmol) are weighed in a 250 mL round-bottomed flask, and then, concentrated H_2O_2 (30% in H_2O, 110.7 g, 976.8 mmol) is added. The mixture is allowed to stir at room temperature for 24 h, progressively turning from yellow to white. Reaction progress can be monitored by TLC (heptane/AcOEt 7:3). The mixture is filtered on a fritted silica funnel, washed with water (40 mL), and dried at 60 °C under vacuum until weight stabilization. White powder, 11.579 g, 98.7% yield. mp 232−234 °C (lit. 231−232 °C). ^{1}H NMR (400 MHz, $CDCl_3$): δ 7.83−7.79 (m, 4H), 7.66−7.62 (m, 2H), 7.55−7.51 (m, 2H) ppm.

9,9′-Spirobifluorene (4). Dibenzothiophene-S,S-dioxide 7 (2.000 g, 9.249 mmol), fluorene (2.306 g, 13.87 mmol), 18-crown-6 (0.245 g, 0.925 mmol), and finely ground KOH (85%, 2.442 g, 37.00 mmol) are weighed in a two-necked 100 mL round-bottomed flask, equipped with a reflux condenser. The system is put under a nitrogen atmosphere by means of a Schlenk line. Here, 1 mL of diglyme is added, and the flask is heated to 115 °C for 3 h, observing the color turning from yellowish to purple. The reaction is further heated to 160 °C for 21 h. The reaction is quenched by addition of 3.5 mL of degassed methanol and refluxed until the disappearance of the purple color. Upon cooling to room temperature, the reaction mixture is filtered on a pad of Celite (5 g) using toluene as the eluent (50 mL). The solvent is evaporated under reduced pressure, and the obtained raw mixture is purified by sublimation to separate the product from unreacted excess fluorene. Here, 2.418 g of product (yellow powder, 82.7%) and 0.998 g of fluorene are recovered. 194−196 °C (lit. 198−199 °C). ^{1}H NMR (400 MHz, $CDCl_3$): δ 7.85 (d, J = 7.6 Hz, 4H), 7.37 (m, 4H), 7.11 (m, 4H), 6.73 (d, J = 7.6 Hz, 4H) ppm. ^{13}C NMR (100 MHz, $CDCl_3$): δ 148.76, 141.76, 127.80, 127.68, 124.02, 119.96, 66.02 ppm.

2,2′,7,7′-Tetrabromo-9,9′-spirobifluorene (5). In a two-necked 100 mL round-bottomed flask equipped with dropping funnel, 9,9′-spirobifluorene **4** (1.850 g, 5.849 mmol) is suspended in aqueous 4% Dowfax 3B2 (9.00 g). Concentrated H_2O_2 (30% in H_2O, 4.0 mL, 5.76 g) is added, and the reaction flask is cooled to 0 °C by mean of an ice bath. Bromine (5.607 g, 35.09 mmol) is therefore added dropwise in 20 min. After 40 more minutes, the ice bath is removed, and the reaction is allowed to stir at room temperature overnight. After 16 h, the reaction is quenched by addition of aqueous 10% $NaHSO_3$ (30 g), observing the disappearance of the red color. The mixture is filtered on a fritted silica funnel, and the as-obtained yellowish powder is dried at 60 °C under vacuum. The raw mixture is purified by Soxhlet extraction using ethanol (50 mL) as the solvent. Both the undissolved material in the thimble and the crystallized material in the ethanol are recovered as pure product. White powder, 3.030 g, 82.0%. mp 398−399 °C (lit. 395−400 °C). ^{1}H NMR (400 MHz, CDCl3): δ 7.68 (d, J = 8.2 Hz, 4H), 7.54 (dd, J = 8.1, 1.8 Hz, 4H), 6.83 (d, J = 1.7 Hz, 4H) ppm. ^{13}C NMR (100 MHz, $CDCl_3$): δ 148.79, 139.55, 131.76, 127.33, 122.17, 121.68, 66.25 ppm.

2,2′,7,7′-Tetrakis(N,N-di-*p*-methoxyphenylamine)9,9′-spirobifluorene (Spiro-OMeTAD). 2,2′,7,7′-Tetrabromo-9,9′-spirobifluorene (316 mg, 0.500 mmol), 4,4′-dimethoxydiphenylamine (573 mg, 2.50 mmol), $Pd(OAc)_2$ (9.0 mg, 0.040 mmol), XPhos (38.1 mg, 0.080 mmol), K_3PO_4 (637 mg, 3.00 mmol), and PEG 2000 dimethyl ether (38 mg) are weighed in a 10 mL Schlenk tube. The system is put under a nitrogen atmosphere by mean of a Schlenk line. Toluene (0.5 mL) is added, and the reaction is heated to 110 °C for 24 h. Reaction progress can be monitored by TLC (heptane/AcOEt 7:3, R_f = 0.19). The reaction is warmed to room temperature, and 3 mL of toluene is added. The soluble fraction is added dropwise to 20 mL of methanol, and the precipitate is collected by filtration and washed with 5 mL of methanol. The powder is dried at 60 °C under vacuum and then subjected to a further purification to remove the Pd catalyst.

Raw Sample. The raw sample is purified by filtration over a pad of silica (15 g) using AcOEt as the eluent (180 mL). Dark yellow powder, 577 mg, 94% yield (purity 95% according to ^{1}H NMR, Figures S14 and S15).

C-Filt Sample. The C-filt sample is purified by filtration over decolorizing DARCO carbon at −12 °C, using AcOEt/dioxolane 6:4 as the eluent (this operation is described in detail in Section 5). Pale yellow powder, 459 mg, 75% yield. ^{1}H NMR (400 MHz, C_6D_6): δ 7.13 (s, 4H), 7.06 (d, J = 2.0 Hz, 4H), 7.02 (m, 16H), 6.97 (dd, J = 8.3, 2.1 Hz, 4H), 6.73 (m, 16H), 3.25 (s, 24H) ppm.

RESULTS AND DISCUSSION

Green Synthesis of 9,9′-Spiro-bifluorene. Aiming at dramatically improving all the aspects of the synthetic access to

Table 1. Tested Conditions for Synthesis of 9,9′-Spirobifluorene

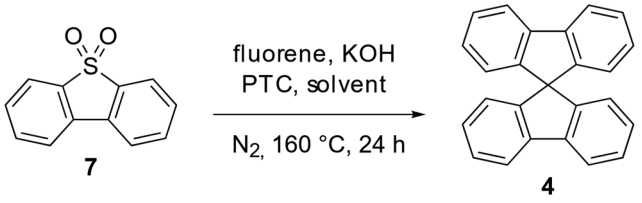

Entry	Solvent	Phase transfer catalyst	Yield (%)
1	Anisole	PEG2000OMe	52
2	Anisole	18-crown-6	56
3	Proglyde	PEG2000OMe	56
4	Proglyde	18-crown-6	60
5	Diglyme	18-crown-6	83

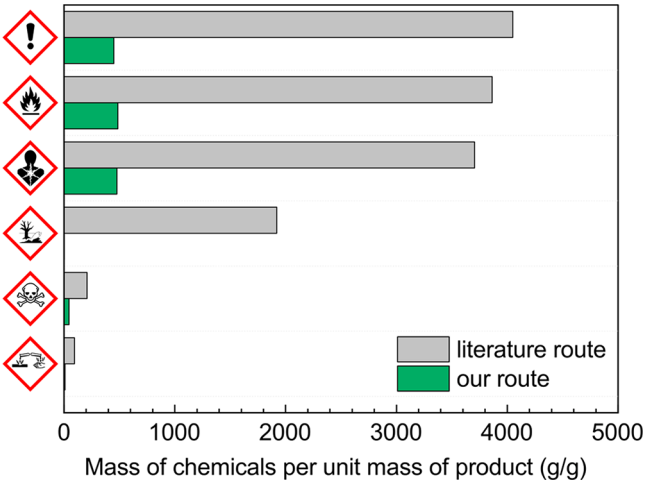

Figure 2. Amount of chemicals ranked by chemical hazards associated with the different synthetic routes.

Spiro-OMeTAD, we employed a variety of green chemistry approaches enabling (a) a reduction of the E-Factor by one order of magnitude, (b) removal of all hazardous and pyrophoric materials, (c) reduction to a bare minimum of

https://doi.org/10.1021/acssuschemeng.2c00493
ACS Sustainable Chem. Eng. 2022, 10, 4750−4757

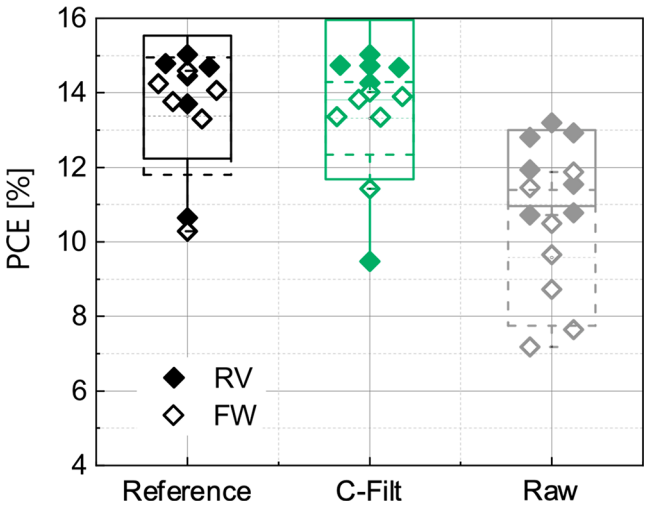

Figure 3. Power conversion efficiency (PCE) of PVK cells fabricated with commercial Spiro-OMeTAD (reference), or with **Raw** and **C-Filt** samples. Photovoltaic parameters extracted either from the reverse (RV) current−voltage scan (from V_{OC} to V = 0) and the forward (FW) scan (from V = 0 to V_{OC}). Boxes indicate the standard deviation and mean value of the results in the RV (continuous line) and FW scan (dotted line).

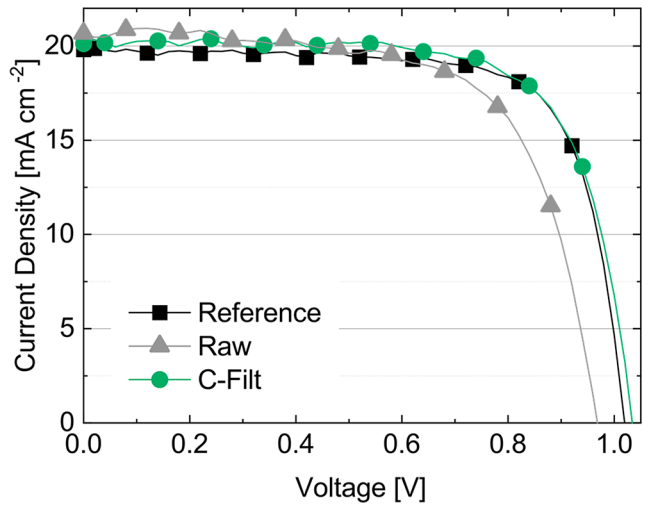

Figure 4. Current density vs voltage curves of the best glass/ITO/SnO_2/FAMACs/HTM/Au cells with commercial Spiro-OMeTAD HTM (reference), or with the newly synthesized spiro-type HTM either purified by charcoal filtration (**C-Filt**) or silica filtration (**Raw**).

organic solvents employed, (d) resource efficient purification, and (e) ease of scale up.

First, we tackled the preparation of 9,9′-spirobifluorene **4**. This is a key material not only for the preparation of Spiro-OMeTAD but for the whole family of spirobifluorene-emitting molecules and polymers developed for OLED fabrication.[24−27] The only documented alternative to the reaction of either the Grignard or the organolithium derivatives prepared from 2-bromo or 2-iododiphenyl with fluorenone was recently reported by Yorimitzu et al.. The reaction of fluorene and dibenzothiophene-S,S-dioxide (**7**) in the presence of KN-$(SiMe_3)_2$ as the base in anhydrous dioxane at 150 °C for 16 h gives **4** in 45% yield after chromatographic purification.[28]

We thought this synthesis promising as **7** can be prepared by the quantitative oxidation of dibenzothiophene by hydrogen peroxide in the presence of catalytic H_2WO_4. Dibenzothiophene is a widely available petrochemical raw material. After careful optimization of reaction conditions (Table 1), we found out that the reaction of **7** with excess fluorene under solid−liquid phase transfer catalysis (SL-PTC) with KOH and 18-crown-6 as the phase transfer catalyst (PTC) in refluxing diethylene glycol dimethyl ether (diglyme) yields **4** in 83% yield. The use of SL-PTC conditions enhances the basicity of a safe and inexpensive inorganic base (KOH 85%) enabling the substitution of the hazardous potassium bis(trimethylsilyl)-amide (KHDMS) and the need of anhydrous solvents. The benefits in terms of cost (no dehydration required) and ease of operation (no dry atmosphere required) are substantial, particularly while scaling up. Moreover, no chromatographic purification is required as the crude reaction mixture is simply filtered through a pad of Celite and evaporated. Excess fluorene contaminating the crude can be removed via vacuum sublimation and recycled.

As very little solvent is required, the E-factor of this step is 23.0. On a large scale, the reaction would not require any solvent as the molten excess fluorene is a good enough solvent. On a lab scale, such a solution is unpractical due to the tendency of the latter to sublime away from the reaction mixture. The reprotoxic diethylene glycol dimethyl ether can be replaced with eco-friendly proglyde (di(propylene glycol) dimethyl ether, mixture of isomers) at the expense of a modest reduction of the yield from 83% to 60% (Table 1, entry 4).

Bromination of 9,9′-Spirobifluorene under Micellar Catalysis and Buchwald−Hartwig Amination. For the bromination of **4**, we evaluated water as the reaction medium, bromine as the electrophile, and an oxidizer. The presence of the oxidizer is necessary to oxidize the HBr formed in the reaction back to Br_2, thus improving the overall atom economy of the rection.

We tested both "on water" catalysis,[29] working with a suspension of **4** in aqueous Oxone, and micellar catalysis, in this case using a 4 wt % solution of Dowfax 3B2 and H_2O_2 (Table S6). Dowfax 3B2 is an industrial anionic surfactant, very cheap and freely soluble in water even at 0 °C, the temperature required to control the regioselectivity of bromination. Both "on water"- and micellar-catalyzed reactions gave almost quantitative conversion. The use of Oxone in water led to the formation of oxidation byproducts substantially impacting on the reaction yield. Conversely the micellar reaction performed in aqueous Dowfax 3B2 enables the straightforward isolation of the target regioisomer in 82% yield by simple filtration of the crude reaction mixture followed by extractive (Soxhlet) crystallization. The literature procedure (requiring the use of chloroform as the solvent) remains more efficient in terms of yield,[12] yet we reduced the E-factor of the single step from 225 to 29.3, and we did not use toxic solvents.

The final step requires the Buchwald-Hartwig (B−H) palladium-catalyzed amination of **5**. B−H amination is among the many transformations reported to be particularly efficient under micellar catalysis conditions.[30−33] We tested the reaction under several distinct micellar conditions (details are included in Table S7), with best results obtained when working with aqueous 2 wt % cetyltrimethylammonium bromide (CTAB) in a 9:1 vol/vol mixture with toluene. Under such conditions, we obtained Spiro-OMeTAD in 32% yield after chromatographic purification. We got much better results by completely removing the solvent, thus carrying out the reaction in the melt using 6 equiv of the 4,4′-dimethoxydiphenylamine.

https://doi.org/10.1021/acssuschemeng.2c00493
ACS Sustainable Chem. Eng. 2022, 10, 4750−4757

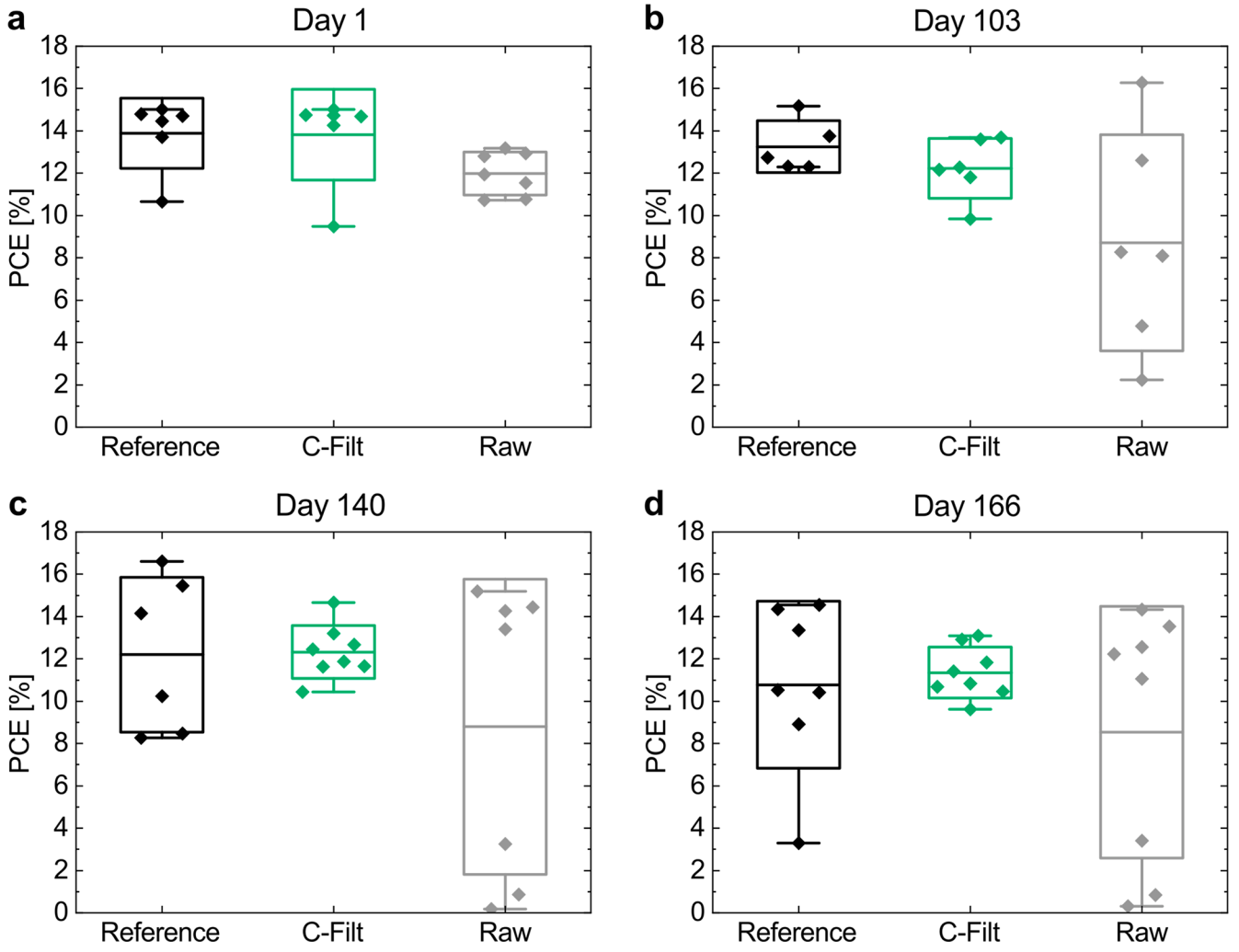

Figure 5. Box charts illustrating the statistical distribution of power conversation efficiency of perovskite solar cells at (a) day 1, (b) day 103, (c) day 140, and (d) day 166. Between measurements, samples were stored in the dark in a box with relative humidity (RH) in the 30%−40% range. Measurements were performed under standard test conditions (STC, 25 °C, 1000 W/m^2 irradiance, air mass 1.5 (AM1.5) spectrum), and the photovoltaic parameter was extracted from the reverse scan at a rate of 33 mV/s.

The reaction proceeds with complete conversion of starting bromide under a standard laboratory environment and with an isolated yield of 60%, after column chromatography. We further improved the results by the addition of a 25 wt % of toluene with respect to the total amount of reagents and near stoichiometric amine. The NMR analysis of the crude reaction mixture evidenced the expected product, barely contaminated by small amounts of tris-aminated intermediate, still bearing one bromine residue, and 4,4′-dimethoxydiphenylamine. After reprecipitation of the crude in methanol, we carried out a filtration through a pad of silica to remove the catalyst, affording the product in 95% purity (in the following section, such a sample is identified as **Raw**). The ICP characterization of traces impurities in the **Raw** samples shows 65 ppm of remaining Pd.

Solvent Efficient Purification of Spiro-OMeTAD. To reduce the amount of Pd contaminant and remove the other byproducts (trisubstituted intermediate and amine), we devised a simple and solvent efficient nonchromatographic purification method involving a cold filtration of a concentrated AcOEt:dioxolane 6:4 vol:vol solution of the crude through a pad of carbon black. We selected such a stationary phase according to the known affinity of carbon black for halogenated aromatics as well as for palladium. The process enables the reduction of the Pd contamination below the sensitivity level (1 ppb) of ICP (this sample was identified as **C-Filt**) and allows one to increase purity from 95% to >99% (according to NMR characterization).

Scheme 1 summarizes the conditions and the corresponding overall metrics (starting from commercial raw materials) of reference commercial Spiro-OMeTAD and **C-Filt**. Under the best experimental conditions and including purification, we managed to reduce the overall E-factor from 5299 to 555. We also dramatically improved safety. Figure 2 shows the health and safety risks associated with the chemicals used in the different synthetic routes. Our route enables a critical reduction of all hazardous chemicals and a complete removal of the particularly obnoxious halogenated solvents and hazardous organometallic species.

Performances of Spiro-OMeTAD Samples in Perovskite Solar Cells. We evaluated the HTL performances of all materials in perovskite-based solar cells. We fabricated triple cation perovskite cells with glass/ITO/SnO_2/$Cs_{0.06}FA_{0.78}MA_{0.16}Pb(I_{0.84}Br_{0.16})_3$ (FAMACs)/ HTM/Au ar-

https://doi.org/10.1021/acssuschemeng.2c00493
ACS Sustainable Chem. Eng. 2022, 10, 4750−4757

chitecture according to previously optimized fabrication procedures,[34] and we characterized comparative performances and stability according to the protocols proposed by the International Summit on OPV Stability (ISOS)-D-1 shelf testing conditions.

The three materials are identical from the point of view of UV−vis absorption properties (Figure S5). Figure 3 shows the PCE of cells having the structure glass/ITO/SnO_2/FAMACs/HTM/Au, where the HTM is either the reference commercial Spiro-OMeTAD (purchased by Borun New Material Technology LTD) or the newly synthesized materials, measured both from the reverse (RV) current−voltage scan (from V_{OC} to $V = 0$) and the forward (FW) current−voltage scan (from $V = 0$ to V_{OC}).

Reference and **C-Filt** samples behave identically within the experimental error (13.9% and 13.8% average efficiency from the reverse scan, respectively), while the **Raw** derivative provides sizably poorer performance (12% average PCE). The best efficiencies achieved were 15.0% for both the cells with **C-Filt** and reference Spiro-OMeTAD, and 13.2% for the **Raw** material. These values are close to average values of a large, scattered database of over 42,400 cells collected by Jacobsson et al.[35] Future improvements in performance can be sought by controlling conditions during device fabrication, including engineering composite electron transport layers that can boost PCEs significantly further.[36,37]

The lower efficiencies of **Raw** cells, as well as higher hysteresis, are mainly the result of lower fill factors (Table S9 and Figure S6) and slightly lower open circuit voltages, possibly resulting from the presence of traces of palladium, as well as other contaminants in these nonpurified HTLs. Current−voltage characteristics of the best cells for each HTL are reported in Figure 4.

Figure 5 shows that the shelf life stability of the solar cells with our **C-Filt** sample is as good as the commercial solar grade material and even superior, especially in reproducibility, over a period of 166 days where the cells were stored in the dark in a controlled environment with relative humidity between 30% and 40%.

After 166 days, **C-Filt** devices are still essentially unchanged, whereas reference devices show a significantly larger scatter in the results and a PCE reduced to 77.5% of the day 1 value. Within the same time frame, **C-Filt** devices preserved 82.2% of their original efficiency.

CONCLUSIONS

We have developed a new, green chemistry compliant, and economically advantageous protocol for the preparation of Spiro-OMeTAD, a key enabling material for the perovskite solar cells technology.

The new protocol is advantageous over the existing ones in terms of removal of hazardous chemicals, reduction of wastes, overall efficiency, and purity of the final material. The key steps of the new synthesis are a more direct access to the key intermediate 9,9′-spirobifluorene, a micellar-catalyzed bromination of the same in a water solution of surfactants and a Buchwald−Hartwig amination performed in almost solventless conditions. We have also developed a purification protocol involving minimum amounts of organic solvents and providing samples whose performances in perovskite cell devices are better, particularly in terms of reproducibility and durability, with respect to those afforded by commercially available reference samples. The effect is possibly connected with a particularly low level of contamination from traces of metal catalysts and intermediates of incomplete B−H amination. The new protocol is directly scalable and could contribute to significantly reducing the cost and overall environmental impact of the rapidly emerging perovskite photovoltaic technology.

ASSOCIATED CONTENT

Supporting Information

The Supporting Information is available free of charge at https://pubs.acs.org/doi/10.1021/acssuschemeng.2c00493.

Details on selection and calculation of green metrics employed and of cost model selected. Details on calculations of cost and E-factor according to data discussed in ref 9 (https://doi.org/10.1021/acsnano.0c08903). Details on calculation of E-Factor and cost according to procedure described in this paper. Assessment of alternative synthetic routes toward 9,9′-spirobifluorene and 2,2′,7,7′-tetrabromo-9,9′-spirobifluorene. Developed alternative synthetic conditions for synthesis of 2,2′,7,7′-tetrabromo-9,9′-spirobifluorene and Spiro-OMeTAD. Detailed description of purification procedure requiring filtration over DARCO charcoal. Further characterizations of perovskite solar cells. Copies of ^1H and ^{13}C NMR spectra of all compounds (PDF)

AUTHOR INFORMATION

Corresponding Author

Luca Beverina − *Department of Materials Science, University of Milano-Bicocca and INSTM, I-20125 Milan, Italy;* orcid.org/0000-0002-6450-545X; Email: luca.beverina@unimib.it

Authors

Sara Mattiello − *Department of Materials Science, University of Milano-Bicocca and INSTM, I-20125 Milan, Italy;* orcid.org/0000-0002-2907-0964

Giulia Lucarelli − *CHOSE (Centre for Hybrid and Organic Solar Energy), Department of Electronic Engineering, University of Rome Tor Vergata, I-00133 Rome, Italy*

Adiel Calascibetta − *Department of Materials Science, University of Milano-Bicocca, I-20125 Milan, Italy*

Lorenzo Polastri − *Department of Materials Science, University of Milano-Bicocca, I-20125 Milan, Italy*

Erika Ghiglietti − *Department of Materials Science, University of Milano-Bicocca, I-20125 Milan, Italy*

Suresh Kumar Podapangi − *CHOSE (Centre for Hybrid and Organic Solar Energy), Department of Electronic Engineering, University of Rome Tor Vergata, I-00133 Rome, Italy*

Thomas M. Brown − *CHOSE (Centre for Hybrid and Organic Solar Energy), Department of Electronic Engineering, University of Rome Tor Vergata, I-00133 Rome, Italy;* orcid.org/0000-0003-2141-3587

Mauro Sassi − *Department of Materials Science, University of Milano-Bicocca and INSTM, I-20125 Milan, Italy;* orcid.org/0000-0002-5529-6449

Complete contact information is available at: https://pubs.acs.org/10.1021/acssuschemeng.2c00493

Author Contributions

S.M. and L.B. wrote the manuscript. A.M.C, L.P., E.G. and M.S. contributed equally to the synthetic efforts. G.L. and S.K.P. contributed equally to devices assembly and characterization. L.B. and T.M.B. conceptualized the study and coordinated the work.

Notes

The authors declare no competing financial interest.

■ ACKNOWLEDGMENTS

L.B., M.S., and S.M. gratefully acknowledge the financial contribution from MIUR under Grant "Dipartimenti di Eccellenza 2017 Project−Materials for Energy". All authors gratefully acknowledge the financial contribution from MIUR under Grant PRIN2017 BOOSTER (2017YXX8AZ)

■ REFERENCES

(1) Lee, M. M.; Teuscher, J.; Miyasaka, T.; Murakami, T. N.; Snaith, H. J. Efficient Hybrid Solar Cells Based on Meso-Superstructured Organometal Halide Perovskites. *Science* **2012**, *338* (6107), 643−647.

(2) Jeong, J.; Kim, M.; Seo, J.; Lu, H.; Ahlawat, P.; Mishra, A.; Yang, Y.; Hope, M. A.; Eickemeyer, F. T.; Kim, M.; Yoon, Y. J.; Choi, I. W.; Darwich, B. P.; Choi, S. J.; Jo, Y.; Lee, J. H.; Walker, B.; Zakeeruddin, S. M.; Emsley, L.; Rothlisberger, U.; Hagfeldt, A.; Kim, D. S.; Grätzel, M.; Kim, J. Y. Pseudo-Halide Anion Engineering for α-FAPbI 3 Perovskite Solar Cells. *Nature* **2021**, *592* (7854), 381−385.

(3) Bakr, Z. H.; Wali, Q.; Fakharuddin, A.; Schmidt-Mende, L.; Brown, T. M.; Jose, R. Advances in Hole Transport Materials Engineering for Stable and Efficient Perovskite Solar Cells. *Nano Energy* **2017**, *34*, 271−305.

(4) Krüger, J.; Bach, U.; Grätzel, M. Modification of TiO2 Heterojunctions with Benzoic Acid Derivatives in Hybrid Molecular Solid-State Devices. *Adv. Mater.* **2000**, *12* (6), 447−451.

(5) Bach, U.; Tachibana, Y.; Moser, J.-E.; Haque, S. A.; Durrant, J. R.; Grätzel, M.; Klug, D. R. Charge Separation in Solid-State Dye-Sensitized Heterojunction Solar Cells. *J. Am. Chem. Soc.* **1999**, *121* (32), 7445−7446.

(6) Ren, G.; Han, W.; Deng, Y.; Wu, W.; Li, Z.; Guo, J.; Bao, H.; Liu, C.; Guo, W. Strategies of Modifying Spiro-OMeTAD Materials for Perovskite Solar Cells: A Review. *J. Mater. Chem. A* **2021**, *9* (8), 4589−4625.

(7) Rodríguez-Seco, C.; Cabau, L.; Vidal-Ferran, A.; Palomares, E. Advances in the Synthesis of Small Molecules as Hole Transport Materials for Lead Halide Perovskite Solar Cells. *Acc. Chem. Res.* **2018**, *51* (4), 869−880.

(8) Dey, A.; Ye, J.; De, A.; Debroye, E.; Ha, S. K.; Bladt, E.; Kshirsagar, A. S.; Wang, Z.; Yin, J.; Wang, Y.; Quan, L. N.; Yan, F.; Gao, M.; Li, X.; Shamsi, J.; Debnath, T.; Cao, M.; Scheel, M. A.; Kumar, S.; Steele, J. A.; Gerhard, M.; Chouhan, L.; Xu, K.; Wu, X.; Li, Y.; Zhang, Y.; Dutta, A.; Han, C.; Vincon, I.; Rogach, A. L.; Nag, A.; Samanta, A.; Korgel, B. A.; Shih, C.-J.; Gamelin, D. R.; Son, D. H.; Zeng, H.; Zhong, H.; Sun, H.; Demir, H. V.; Scheblykin, I. G.; Mora-Seró, I.; Stolarczyk, J. K.; Zhang, J. Z.; Feldmann, J.; Hofkens, J.; Luther, J. M.; Pérez-Prieto, J.; Li, L.; Manna, L.; Bodnarchuk, M. I.; Kovalenko, M. V.; Roeffaers, M. B. J.; Pradhan, N.; Mohammed, O. F.; Bakr, O. M.; Yang, P.; Müller-Buschbaum, P.; Kamat, P. V.; Bao, Q.; Zhang, Q.; Krahne, R.; Galian, R. E.; Stranks, S. D.; Bals, S.; Biju, V.; Tisdale, W. A.; Yan, Y.; Hoye, R. L. Z.; Polavarapu, L. State of the Art and Prospects for Halide Perovskite Nanocrystals. *ACS Nano* **2021**, *15*, 10775.

(9) Petrus, M. L.; Bein, T.; Dingemans, T. J.; Docampo, P. A Low Cost Azomethine-Based Hole Transporting Material for Perovskite Photovoltaics. *J. Mater. Chem. A* **2015**, *3* (23), 12159−12162.

(10) Saliba, M.; Orlandi, S.; Matsui, T.; Aghazada, S.; Cavazzini, M.; Correa-Baena, J.-P.; Gao, P.; Scopelliti, R.; Mosconi, E.; Dahmen, K.-H.; De Angelis, F.; Abate, A.; Hagfeldt, A.; Pozzi, G.; Graetzel, M.; Nazeeruddin, M. K. A Molecularly Engineered Hole-Transporting Material for Efficient Perovskite Solar Cells. *Nat. Energy* **2016**, *1* (2), 15017.

(11) Kamino, B. A.; Mills, B.; Reali, C.; Gretton, M. J.; Brook, M. A.; Bender, T. P. Liquid Triarylamines: The Scope and Limitations of Piers-Rubinsztajn Conditions for Obtaining Triarylamine-Siloxane Hybrid Materials. *J. Org. Chem.* **2012**, *77* (4), 1663−1674.

(12) Wu, R.; Schumm, J. S.; Pearson, D. L.; Tour, J. M. Convergent Synthetic Routes to Orthogonally Fused Conjugated Oligomers Directed toward Molecular Scale Electronic Device Applications. *J. Org. Chem.* **1996**, *61* (20), 6906−6921.

(13) Poriel, C.; Ferrand, Y.; Juillard, S.; Le Maux, P.; Simonneaux, G. Synthesis and Stereochemical Studies of Di and Tetra 9,9′-Spirobifluorene Porphyrins: New Building Blocks for Catalytic Material. *Tetrahedron* **2004**, *60* (1), 145−158.

(14) Jeon, N. J.; Lee, H. G.; Kim, Y. C.; Seo, J.; Noh, J. H.; Lee, J.; Seok, S. I. *O* -Methoxy Substituents in Spiro-OMeTAD for Efficient Inorganic-Organic Hybrid Perovskite Solar Cells. *J. Am. Chem. Soc.* **2014**, *136* (22), 7837−7840.

(15) Sheldon, R. A. Metrics of Green Chemistry and Sustainability: Past, Present, and Future. *ACS Sustainable Chem. Eng.* **2018**, *6* (1), 32−48.

(16) Lipshutz, B. H.; Ghorai, S. Transitioning Organic Synthesis from Organic Solvents to Water. What's Your E Factor? *Green Chem.* **2014**, *16* (8), 3660−3679.

(17) Sheldon, R. A. The E Factor 25 Years on: The Rise of Green Chemistry and Sustainability. *Green Chem.* **2017**, *19* (1), 18−43.

(18) Ansari, T. N.; Gallou, F.; Handa, S. Cross-couplings in Water: A Better Way to Assemble New Bonds. In *Organometallic Chemistry in Industry: A Practical Approach*, 1st ed.; Wiley-VCH Verlag GmbH & Co, 2020: pp 203−238.

(19) Takale, B. S.; Thakore, R. R.; Casotti, G.; Li, X.; Gallou, F.; Lipshutz, B. H. Mild and Robust Stille Reactions in Water Using Ppm Levels of a New Triphenylphosphine-Based Palladacycle. *Angew. Chem., Int. Ed.* **2021**, *60* (8), 4158−4163.

(20) Lipshutz, B. H.; Ghorai, S.; Cortes-Clerget, M. The Hydrophobic Effect Applied to Organic Synthesis: Recent Synthetic Chemistry "in Water. *Chem.—Eur. J.* **2018**, *24* (26), 6672−6695.

(21) Sassi, M.; Mattiello, S.; Beverina, L. Syntheses of Organic Semiconductors in Water. Recent Advancement in the Surfactants Enhanced Green Access to Polyconjugated Molecules. *Eur. J. Org. Chem.* **2020**, *2020* (26), 3942−3953.

(22) Martins, M. A. P.; Frizzo, C. P.; Moreira, D. N.; Buriol, L.; Machado, P. Solvent-Free Heterocyclic Synthesis. *Chem. Rev.* **2009**, *109* (9), 4140−4182.

(23) Usluer, Ö.; Abbas, M.; Wantz, G.; Vignau, L.; Hirsch, L.; Grana, E.; Brochon, C.; Cloutet, E.; Hadziioannou, G. Metal Residues in Semiconducting Polymers: Impact on the Performance of Organic Electronic Devices. *ACS Macro Lett.* **2014**, *3* (11), 1134−1138.

(24) Poriel, C.; Sicard, L.; Rault-Berthelot, J. New Generations of Spirobifluorene Regioisomers for Organic Electronics: Tuning Electronic Properties with the Substitution Pattern. *Chem. Commun.* **2019**, *55* (95), 14238−14254.

(25) Poriel, C.; Rault-Berthelot, J. Structure-Property Relationship of 4-Substituted-Spirobifluorenes as Hosts for Phosphorescent Organic Light Emitting Diodes: An Overview. *J. Mater. Chem. C* **2017**, *5* (16), 3869−3897.

(26) Yang, X.; Xu, X.; Zhou, G. Recent Advances of the Emitters for High Performance Deep-Blue Organic Light-Emitting Diodes. *J. Mater. Chem. C* **2015**, *3* (5), 913−944.

(27) Sicard, L. J.; Li, H.-C.; Wang, Q.; Liu, X.-Y.; Jeannin, O.; Rault-Berthelot, J.; Liao, L.-S.; Jiang, Z.-Q.; Poriel, C. C1-Linked Spirobifluorene Dimers: Pure Hydrocarbon Hosts for High-Performance Blue Phosphorescent OLEDs. *Angew. Chem., Int. Ed.* **2019**, *58* (12), 3848−3853.

(28) Bhanuchandra, M.; Yorimitsu, H.; Osuka, A. Synthesis of Spirocyclic Diarylfluorenes by One-Pot Twofold SNAr Reactions of Diaryl Sulfones with Diarylmethanes. *Org. Lett.* **2016**, *18* (3), 384−387.

https://doi.org/10.1021/acssuschemeng.2c00493
ACS Sustainable Chem. Eng. 2022, 10, 4750−4757

(29) Narayan, S.; Muldoon, J.; Finn, M. G.; Fokin, V. V.; Kolb, H. C.; Sharpless, K. B. On Water": Unique Reactivity of Organic Compounds in Aqueous Suspension. *Angew. Chem., Int. Ed.* **2005**, *44* (21), 3275−3279.
(30) Nishikata, T.; Lipshutz, B. H. Aminations of Allylic Phenyl Ethers via Micellar Catalysis at Room Temperature in Water. *Chem. Commun.* **2009**, No. 42, 6472.
(31) Vaghi, L.; Sanzone, A.; Sassi, M.; Pagani, S.; Papagni, A.; Beverina, L. Synthesis of Fluorinated Acridines via Sequential Micellar Buchwald-Hartwig Amination/Cyclization of Aryl Bromides. *Synthesis* **2018**, *50* (08), 1621−1628.
(32) Ansari, T. N.; Taussat, A.; Clark, A. H.; Nachtegaal, M.; Plummer, S.; Gallou, F.; Handa, S. Insights on Bimetallic Micellar Nanocatalysis for Buchwald-Hartwig Aminations. *ACS Catal.* **2019**, *9* (11), 10389−10397.
(33) Rooney, M.; Mattiello, S.; Stara, R.; Sanzone, A.; Brazzo, P.; Sassi, M.; Beverina, L. Suzuki-Miyaura Cross-Coupling of Latent Pigments in Water/Toluene Emulsion under Aerobic Atmosphere. *Dyes Pigm.* **2018**, *149*, 893−901.
(34) Taheri, B.; De Rossi, F.; Lucarelli, G.; Castriotta, L. A.; Di Carlo, A.; Brown, T. M.; Brunetti, F. Laser-Scribing Optimization for Sprayed SnO2-Based Perovskite Solar Modules on Flexible Plastic Substrates. *ACS Appl. Energy Mater.* **2021**, *4* (5), 4507−4518.
(35) Jacobsson, T. J.; Hultqvist, A.; García-Fernández, A.; Anand, A.; Al-Ashouri, A.; Hagfeldt, A.; Crovetto, A.; Abate, A.; Ricciardulli, A. G.; Vijayan, A.; Kulkarni, A.; Anderson, A. Y.; Darwich, B. P.; Yang, B.; Coles, B. L.; Perini, C. A. R.; Rehermann, C.; Ramirez, D.; Fairen-Jimenez, D.; Di Girolamo, D.; Jia, D.; Avila, E.; Juarez-Perez, E. J.; Baumann, F.; Mathies, F.; González, G. S. A.; Boschloo, G.; Nasti, G.; Paramasivam, G.; Martínez-Denegri, G.; Näsström, H.; Michaels, H.; Köbler, H.; Wu, H.; Benesperi, I.; Dar, M. I.; Bayrak Pehlivan, I.; Gould, I. E.; Vagott, J. N.; Dagar, J.; Kettle, J.; Yang, J.; Li, J.; Smith, J. A.; Pascual, J.; Jerónimo-Rendón, J. J.; Montoya, J. F.; Correa-Baena, J.-P.; Qiu, J.; Wang, J.; Sveinbjörnsson, K.; Hirselandt, K.; Dey, K.; Frohna, K.; Mathies, L.; Castriotta, L. A.; Aldamasy, M. H.; Vasquez-Montoya, M.; Ruiz-Preciado, M. A.; Flatken, M. A.; Khenkin, M. V.; Grischek, M.; Kedia, M.; Saliba, M.; Anaya, M.; Veldhoen, M.; Arora, N.; Shargaieva, O.; Maus, O.; Game, O. S.; Yudilevich, O.; Fassl, P.; Zhou, Q.; Betancur, R.; Munir, R.; Patidar, R.; Stranks, S. D.; Alam, S.; Kar, S.; Unold, T.; Abzieher, T.; Edvinsson, T.; David, T. W.; Paetzold, U. W.; Zia, W.; Fu, W.; Zuo, W.; Schröder, V. R. F.; Tress, W.; Zhang, X.; Chiang, Y.-H.; Iqbal, Z.; Xie, Z.; Unger, E. An Open-Access Database and Analysis Tool for Perovskite Solar Cells Based on the FAIR Data Principles. *Nat. Energy* **2022**, *7* (1), 107−115.
(36) Dagar, J.; Castro-Hermosa, S.; Lucarelli, G.; Zampetti, A.; Cacialli, F.; Brown, T. M. Low-Temperature Solution-Processed Thin SnO2/Al2O3 Double Electron Transport Layers Toward 20% Efficient Perovskite Solar Cells. *IEEE Journal of Photovoltaics* **2019**, *9* (5), 1309−1315.
(37) Dagar, J.; Castro-Hermosa, S.; Lucarelli, G.; Cacialli, F.; Brown, T. M. Highly Efficient Perovskite Solar Cells for Light Harvesting under Indoor Illumination via Solution Processed SnO2/MgO Composite Electron Transport Layers. *Nano Energy* **2018**, *49*, 290−299.

https://doi.org/10.1021/acssuschemeng.2c00493
ACS Sustainable Chem. Eng. 2022, 10, 4750−4757